

Revisiting Recurrent Reinforcement Learning with Memory Monoids

Steven Morad¹ Chris Lu² Ryan Kortvelesy¹ Stephan Liwicki³ Jakob Foerster² Amanda Prorok¹

Abstract

In RL, memory models such as RNNs and transformers address Partially Observable Markov Decision Processes (POMDPs) by mapping trajectories to latent Markov states. Neither model scales particularly well to long sequences, especially compared to an emerging class of memory models sometimes called linear recurrent models. We discover that the recurrent update of these models is a *monoid*, leading us to formally define a novel *memory monoid* framework. We revisit the traditional approach to batching in recurrent RL, highlighting both theoretical and empirical deficiencies. Leveraging the properties of memory monoids, we propose a new batching method that improves sample efficiency, increases the return, and simplifies the implementation of recurrent loss functions in RL.

1. Introduction

Reinforcement learning focuses on solving Markov Decision Processes (MDPs), although in many interesting problems we cannot access the Markov state directly. Outside of simulators, we instead receive noisy or ambiguous *observations*, resulting in Partially Observable MDPs.

The standard approach to handling partial observability in model-free RL is to process a sequence of observations into a sequence of latent Markov states using a *memory model* (sometimes called a *sequence model*), such as an RNN or transformer. One can then feed the latent Markov states to a policy and treat the problem as if it were fully observable.

Unfortunately, it is often intractable to train transformers or RNNs over long sequences. In practice, we truncated and zero-pad episodes into *segments*, keeping the sequence length short. Many high-profile works⁴ follow this

segment-based approach, along with seemingly all existing RL libraries⁵.

In search of efficiency, researchers have moved towards a new class of sequence models, sometimes referred to as linear recurrent models or linear transformers⁶. The defining characteristic of these models is their subquadratic time and space complexity over long sequences.

Since these efficient models do not share sequence length limitations with past models, we question *whether the use of segments is still necessary*. After highlighting the empirical and theoretical shortcomings of segments, we propose an alternative batching method. Our method improves sample efficiency across various tasks and memory models, while simplifying implementation.

Contributions

1. We propose the *memory monoid*, a unifying framework for efficient sequence models. In particular, we
 - Reformulate existing sequence models as memory monoids
 - Derive a memory monoid for the discounted return and advantage, leveraging GPU parallelism
 - Discover a method for inline resets for any memory monoid for multi-episode training
2. We investigate the impact that segments have on reinforcement learning. Specifically, we
 - Highlight theoretical shortcomings of sequence truncation and padding, then demonstrate their significant empirical impact
 - Propose a batching method that improves sample efficiency across all tested models and tasks, while also simplifying recurrent loss functions

¹Department of Computer Science and Technology, University of Cambridge ²Department of Engineering Science, University of Oxford ³Toshiba Europe Ltd.. Correspondence to: Steven Morad <sm2558@cam.ac.uk>.

Code available at <https://github.com/proroklab/memory-monoids>. Copyright 2024 by the author(s).

⁴(Hausknecht & Stone, 2015; Kapturowski et al., 2019; Hafner

et al., 2023; Bauer et al., 2023)

⁵RLlib (Liang et al., 2018), StableBaselines3 (Raffin et al., 2021), CleanRL (Huang et al., 2021), SKRL (Serrano-Muñoz et al., 2023), TorchRL (Anonymous, 2024)

⁶State Space Models (Gu et al., 2022), Fast and Forgetful Memory (Morad et al., 2023b), Linear Recurrent Units (Orvieto et al., 2023), RWKV (Peng et al., 2023), RetNet (Anonymous, 2023), Fast Autoregressive Transformer (Katharopoulos et al., 2020)

2. Preliminaries and Background

Consider an MDP $(S, A, R, \mathcal{T}, \gamma)$, where at each timestep t , an agent produces a transition $T = (s, a, r, s')$ from interaction with the environment. $s, s' \in S$ denotes the current and next states and state space, $a \in A$ denotes the action and action space, $R : S \times A \times S \mapsto \mathbb{R}$ denotes the reward function with r as the reward, and $\mathcal{T} : S \times A \mapsto \Delta S$ denotes the state transition matrix (Δ denotes a distribution). In RL, our goal is to learn a stochastic policy parameterized by θ that maps states to action distributions $\pi_\theta : S \mapsto \Delta A$. The agent samples an action from the policy given the current state $a \sim \pi_\theta(s)$, and stochastically transitions to the next state $s' \sim \mathcal{T}(s, a)$, receiving a reward $r = R(s, a, s')$. The optimization objective is to find the policy weights θ that maximize the expected return, discounted by γ : $\mathbb{E}_{a \sim \pi} [\sum_{j=0}^{\infty} \gamma^j r_j]$.

2.1. Rollouts, Causality, and Episode Boundaries

MDPs often have terminal states, so value-based policies introduce the notion of episode termination using the *done flag* $d \in \{0, 1\}$. We denote a terminal state with $d = 1$, signifying that all subsequent rewards are zero. The done flag is stored in the transition $T = (s, a, r, s', d)$.

Although it is conceptually helpful to think in terms of transition tuples, the full transition is not available during inference – we initially receive only the observation, and then we receive the reward, next state, and done flag r, s', d after transitioning to the next state. We find that our formulation is more clear if we introduce a *begin flag* $b \in \{0, 1\}$ that is emitted alongside each observation, and is available during both training and inference. The begin flag b is 1 at the initial timestep of an episode and 0 otherwise. We differentiate between a transition $T = (s, a, r, s', b, d)$ available only during training, and a partial transition $\bar{T} = (s, b)$ available during both inference and training.

At each epoch, we interact with the environment, producing a *rollout* of transitions $\rho = (T_1, T_2, \dots, T_n)$ for training the policy. We may either train on these transitions immediately or store them in a replay buffer for later use.

2.2. Partially Observable Rollouts

In partially observable settings, we can only indirectly measure the Markov state s via the observation $o \sim \mathcal{O}(s)$, following the observation function $\mathcal{O} : S \rightarrow \Delta O$. With the observation replacing the state, interaction with the environment now produces a transition $T = (o, a, r, o', d, b)$ and partial transition $\bar{T} = (o, b)$.

To mitigate partial observability, we summarize a sequence of transitions extending until $d = 1$, also called an episode E , into a latent Markov state. We call these methods mem-

ory models or sequence models, and they may be recurrent. If they are recurrent, their function signature is

$$M : H \times \bar{T} \mapsto H \times S, \quad (1)$$

where H is the set of recurrent states. If they are not recurrent or we wish to abstract away the recurrence, then memory models are simply a mapping from n episode transitions to n Markov states

$$M : \bar{T}^n \mapsto S^n. \quad (2)$$

To correctly estimate the Markov states, the memory model must process all transitions in the entire episode E in sequential order. Each episode E often contains a variable number of transitions, making it difficult to store, batch, or efficiently train over more than one episode at a time.

2.3. On the Efficiency of Sequence Models

The sequence models used in RL are often RNNs or transformers – both of which are intractable for training over long sequences. RNNs cannot be parallelized over the time dimension, and are therefore unable to exploit the parallelism of modern GPUs. Transformer space complexity scales quadratically with sequence length, necessitating large amounts of GPU memory. Recent work on improving transformer efficiency resulted in a number subquadratic-space, time-parallel models, with each parallel thread running in logarithmic time. These models, such as State Space Models (Gu et al., 2021), Linear Transformers (Katharopoulos et al., 2020), Fast Weight Programmers (Schlag et al., 2021), RetNet (Anonymous, 2023), RWKV (Peng et al., 2023), Linear Recurrent Units (Orvieto et al., 2023), or Fast and Forgetful Memory (Morad et al., 2023b) are sometimes called *linear recurrent models* because they usually employ a linear recurrent state update (e.g., $\dot{x} = Cx + c$ where C, c are learned parameters).

3. A Functional Approach to Recurrent Models

As stated in the previous section, most linear recurrent models utilize a linear recurrent state update. This update has a more general form known as a *monoid* (Bourbaki, 1965) – a concept from set theory often used in functional programming.

Definition 3.1. A tuple (H, \bullet, H_I) is a monoid if the following properties hold:

$$\begin{aligned} &\text{The binary operator } \bullet \text{ is associative and closed on } H \\ &(a \bullet b) \bullet c = a \bullet (b \bullet c), \quad \forall (a, b, c) \in H \end{aligned} \quad (3)$$

$$\begin{aligned} &\text{There exists an identity element } H_I \\ &(H_I \bullet a) = (a \bullet H_I) = a, \quad \forall a \in H, H_I \in H, \end{aligned} \quad (4)$$

where \bullet for a single input a is defined as $(\bullet a) = (H_I \bullet a)$.

Unlike prior work on Linear Time Invariant (LTI) models (e.g., State Space Models), the binary operator \bullet *need not be linear or time invariant*. For example, a monoid reformulation of the update rule from a Fast and Forgetful Memory cell (Appendix E, (Morad et al., 2023a)) is both nonlinear and time-dependent: $(A, t) \bullet (A', t') = (A \odot \exp(t'(-|\alpha| \oplus i\omega)) + A', t + t')$, where α, ω are learned vectors and \odot is the Hadamard product.

Any monoid operator \bullet can be parallelized across the time dimension using a parallel scan (Dhulipala et al., 2021). Given a sequence length n , a work-efficient parallel scan known as the Blelloch Scan executes $O(n)$ calls to \bullet in $O(n)$ space to produce n outputs (Blelloch, 1990). With p parallel processors, the parallel time complexity is $O(n/p + \log p)$. For large GPUs where $n = p$, the time complexity becomes $O(\log n)$.

While powerful, standard monoids are defined only over the recurrent state space H . Often, we want to decouple the Markov state space S from the recurrent state space H , as in many cases a low dimensional Markov state could be represented as a function of a higher dimensional recurrent state. We extend the monoid in search of more general sequence models by defining the *memory monoid*.

Definition 3.2. $((H, \bullet, H_I), f, g)$ constitute a memory monoid if (H, \bullet, H_I) defines a monoid and functions f, g are:

An encoder, mapping from a partial transition to the right argument of \bullet (5)

$$f : \bar{T} \mapsto H$$

A decoder, mapping an updated recurrent state and a partial transition to a Markov state (6)

$$g : H \times \bar{T} \mapsto S$$

Recall that a partial transition $\bar{T} = (o, b)$. We define a memory model $M : H \times \bar{T} \mapsto H \times S$ (Equation (1)) using our memory monoid, where M is a sequence of two operations:

Update the recurrent state (7)

$$A' = A \bullet f(\bar{T}), \quad A, A' \in H$$

Produce an output from the updated recurrent state (8)

$$s = g(A', \bar{T}), \quad A' \in H, s \in S.$$

Given n inputs, functions f and g can each be split into n concurrent threads, as f, g have no dependencies on previous sequence elements. Consequently, **all memory monoids have logarithmic time complexity and linear space complexity on the length of the sequence.**⁷

⁷Assuming (1) The binary operator \bullet is constant-time and

3.1. Reformulating Existing Sequence Models

As an exercise in the flexibility and conciseness of our memory monoid, let us reformulate an existing memory model as a memory monoid. The linear transformer from (Katharopoulos et al., 2020) can be reformulated as

$$H = \{(A, a) \mid A \in \mathbb{R}^{j \times k}, a \in \mathbb{R}^j\} \quad (9)$$

$$H_I = (0, 0) \quad (10)$$

$$(A, a) \bullet (A', a') = (A + A', a + a') \quad (11)$$

$$f(o, b) = ((W_k o)(W_v o)^\top, W_k o) \quad (12)$$

$$g((A, a), (o, b)) = \text{MLP}\left(\frac{AW_q o}{a^\top W_q o}\right). \quad (13)$$

Given the $((H, \bullet, H_I), f, g)$ for the linear transformer, we can use M (Definition 3.2) to produce the recurrent states $(A_0, a_0), \dots, (A_n, a_n) = H_I \bullet f(o_0, b_0) \cdots \bullet f(o_n, b_n)$, and from the recurrent states, produce Markov states $s_0, \dots, s_n = g((o_0, b_0), (A_0, a_0)), \dots, g((o_n, b_n), (A_n, a_n))$.

We rewrite the S5 variant of State Space Models (Lu et al., 2023), the Linear Recurrent Unit (Orvieto et al., 2023), and Fast and Forgetful Memory (Morad et al., 2023b) as memory monoids in Appendix E.

3.2. Accelerated Discounted Returns

We find that memory monoids can model other recurrences as well. For example, **we can rewrite the discounted return as a memory monoid, computing it in a GPU-efficient fashion using a high-level framework like JAX** (Bradbury et al., 2018)

Theorem 3.3. *The discounted cumulative return given by*

$$G = \sum_{t=0}^{\infty} \gamma^t r_t \quad (14)$$

is equivalent to computing M (Definition 3.2) over r_1, r_2, \dots for the following memory monoid:

$$H = \{(a, r) \mid a \in [0, 1], r \in \mathbb{R}\} \quad (15)$$

$$H_I = (1, 0) \quad (16)$$

$$(a, r) \bullet (a', r') = (aa', ar' + r) \quad (17)$$

$$f(o, b) = (\gamma, o) \quad (18)$$

$$g((a, r), (o, b)) = r. \quad (19)$$

Proof. See Appendix C. \square

Our experiments show that **executing the return memory monoid on the GPU provides a significant speed up**. In

constant-space, which is the case for all models listed thus far. (2) Our processor has n parallel threads of execution, where n is the length of the sequence.

Appendix D, we prove that Generalized Advantage Estimation (GAE) (Schulman et al., 2016) targets can also be rewritten as a memory monoid. We suspect that other styles of return could also be rewritten in this form.

3.3. Inline Recurrent State Resets

So far, we have assumed that we operate over a single episode using the Blleloch Scan. Consider that in RL, we traditionally train over multiple episodes at once. If we were to concatenate the episodes back-to-back into one long sequence, our binary operator \bullet would cross episode boundaries, feeding information from all prior episodes into the following episodes, and information from all future episodes into preceding episodes.

Fortunately, we can transform any monoid into a *resettable monoid*, enabling resets at episode boundaries. This prevents information from leaking across episodes. We note that the transformed monoid operator is nonlinear, unlike the linear operators present in the S5 or LRU memory monoids. The resettable monoid tracks an additional b term in the recurrent state, corresponding to the begin flag denoting episode boundaries.

Theorem 3.4. *All monoids (H, \bullet, H_I) can be transformed into a resettable monoid (G, \circ, G_I) defined as*

$$G = \{(A, b) \mid A \in H, b \in \{0, 1\}\} \quad (20)$$

$$G_I = (H_I, 0) \quad (21)$$

$$(A, b) \circ (A', b') = ((A \cdot (1 - b') + H_I \cdot b') \bullet A', b \vee b') \quad (22)$$

For a single episode, the A term output by the operator \circ is equivalent to the output of \bullet . Over multiple contiguous episodes, \circ prevents information flow across episode boundaries, replacing the left and right arguments of \bullet with H_I at the boundaries.

Proof. See Appendix C. \square

By transforming (H, \bullet, H_I) from a memory monoid into (G, \circ, G_I) , we no longer require separate time and batch dimensions during training. That is, **with the reset-transformed monoid, we can train over one continuous sequence composed of individual episodes.**

4. Segment-Based Batching

Nearly every RL library⁸ uses *Segment-Based Batching* (SBB) when working with partially observable transitions. SBB will truncate and zero pad episodes so that they can

⁸RLlib (Liang et al., 2018), CleanRL (Huang et al., 2021), StableBaselines3 (Raffin et al., 2021), SKRL (Serrano-Muñoz et al., 2023), TorchRL (Anonymous, 2024)

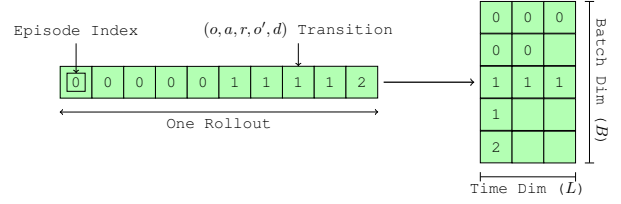


Figure 1. We visualize the Segment-Based Batching approach often used in prior literature. A worker collects episodes, which are split and zero-padded to produce a batch of segments, each with a constant, user-specified segment length L . Episodes exceeding the specified length are broken into multiple segments, preventing backpropagation through time from reaching earlier segments. This approach reduces efficiency, biases normalization methods, and requires specialized recurrent loss functions.

be stacked into a tensor with batch and sequence length dimensions $B \times L$. Each row in this tensor is segment σ containing L transitions.

4.1. Padding, Splitting, and Storage

After collecting episodes E during a rollout, we split E into fragments F such that each F has a maximum length of L . Fragments are zero padded from the right until they are precisely length L , turning them into segments σ and padding masks m . The segments are stacked into a dataset \mathcal{D} , enabling easy batching, storage, and training (Figure 1). We define this approach more accurately in the following paragraphs.

The split function splits a single episode E into one or more fragments F , each of size L except for the final fragment.

$$\begin{array}{ccccccc} F_0 & T_0 & T_1 & \dots & T_{L-1} \\ F_1 & T_L & T_{L+1} & \dots & T_{2(L-1)} \\ \vdots & \vdots & & & \\ F_k & T_{kL} & \dots & & T_n \end{array} = \quad (23)$$

The pad function zero pads a fragment F into a fixed size segment σ and associated mask m denoting the padding elements

$$\sigma, m = \text{pad}(F, L) \quad (24)$$

$$= \text{concat}(F, 0^{L-\text{card}(F)}), \text{concat}(1^{\text{card}(F)}, 0^{L-\text{card}(F)}) \quad (25)$$

Using our split and pad operators, we split and pad each incoming episode, producing one or more segments and associated masks for each episode

$$\begin{bmatrix} \sigma_0, m_0 \\ \vdots \\ \sigma_k, m_k \end{bmatrix} = \text{pad}(F_i, L), \quad \forall F_i \in \text{split}(E, L). \quad (26)$$

We represent our training dataset \mathcal{D} as the concatenation of segments and masks

$$\mathcal{D} = \text{concat} \left(\begin{bmatrix} \sigma_0, m_0 \\ \vdots \\ \sigma_k, m_k \\ \sigma_{k+1}, m_{k+1} \\ \vdots \\ \sigma_j, m_j \\ \vdots \end{bmatrix} \right) = \begin{bmatrix} \sigma_0, m_0 \\ \vdots \\ \sigma_k, m_k \\ \sigma_{k+1}, m_{k+1} \\ \vdots \\ \sigma_j, m_j \\ \vdots \end{bmatrix} \quad (27)$$

During training, we randomly sample rows from \mathcal{D} for minibatching (on-policy) or experience replay (off-policy).

4.2. The Shortcomings of Segments

SBB introduces a number of shortcomings – perhaps the greatest shortcoming with segment-based batching is theoretical in nature. Backpropagation Through Time (BPTT) is truncated at segment boundaries, replacing the true gradient with an estimate.

The true gradient of a recurrent value-based loss function \mathcal{L} parameterized via θ over an episode of length n is

$$\nabla = \frac{\partial \mathcal{L}(\theta, (T_0, T_1, \dots, T_{n-1}))}{\partial \theta}. \quad (28)$$

With length L segments, we estimate the truncated gradient as

$$\nabla_\sigma = \sum_{j=0}^{n/L} \frac{\partial \mathcal{L}(\theta, (T_{jL}, \dots, T_{2(jL-1)}))}{\partial \theta} \quad (29)$$

The gradient is computed independently for each segment. Given two separate segments $\sigma_A, \sigma_B, A < B$, a write to the recurrent state occurring in σ_A impacts a read from the recurrent state in σ_B , however, the gradient with respect to the write parameters will be zero. It is therefore unlikely that temporal dependencies greater than the segment length L can be learned. Prior work (Hausknecht & Stone, 2015; Kapturowski et al., 2019) assumes that $\nabla \approx \nabla_\sigma$, although we are not aware of any theoretical justification for this assumption, as the error between the true and approximated gradient is unbounded.

Beyond incorrectly estimating the gradient, the use of zero padding introduced by segmenting leads to many practical shortcomings. First of all, the zero padding (or in a sparse representation, indices of the non-zero elements) must be stored, taking up additional space. The padding is also fed to the memory model, further wasting time and space. Most RL algorithms must be rewritten to handle padding and an additional time dimension, as evidenced by separate segment-based implementations of RL losses in popular libraries (Raffin et al., 2021; Huang et al., 2021). The amount of zero padding in each sampled batch varies based

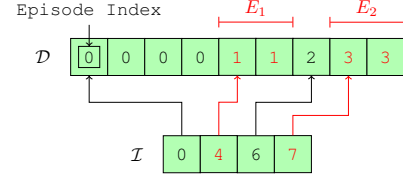


Figure 2. A visualization of sampling in TBB, with a batch size of $B = 4$. Transitions from rollouts are stored in-order in \mathcal{D} , while associated episode begin indices are stored in \mathcal{I} . We sample a train batch by randomly selecting from \mathcal{I} . For example, we might sample 4 from \mathcal{I} , corresponding to E_1 in red. Next, we sample 7 from \mathcal{I} , corresponding to E_2 in red. We concatenate $\mathcal{B} = \text{concat}(E_1, E_2)$ and return the result as a train batch.

on the episode lengths, introducing further issues. Policy updates with less padding will change the weights more than a policy update containing mostly padding. Finally, BatchNorm, InstanceNorm, and other normalization methods compute incorrect statistics due to the padding.

5. Tape-Based Reinforcement Learning

Concerns around SBB stem from the requirement that each sequence is exactly L transitions. However, without this limitation it is not immediately clear how to store and train over episodes. We propose a simple solution: we fold the batch dimension into the time dimension, treating the training data as a single ordered list (the tape). Training over the concatenation of episodes would be intractable for transformers or RNNs (due to poor sequence length scaling), and linear recurrent models (as information leaks between episodes). By combining the efficiency of memory monoids with our resettable transform, we resolve both these issues, enabling us to collapse the batch and time dimensions into a single dimension. We call this approach *Tape-Based Batching* (TBB), providing pseudocode in Appendix G.

5.1. Storage

We maintain ordered lists of transitions \mathcal{D} , and begin indices \mathcal{I} , corresponding to episode boundaries in \mathcal{D} . We update our indices based on the begin flags in the rollout, then append the rollout to our dataset

$$\rho = (T_0, T_1, \dots, T_{n-1}) \quad (30)$$

$$\mathcal{I} = \begin{cases} \text{concat}(\mathcal{I}, (j + \text{card}(\mathcal{D}) \mid b_j, 0 \leq j < n)) & \text{if off-policy} \\ (j \mid b_j, 0 \leq j < n) & \text{if on-policy} \end{cases} \quad (31)$$

$$\mathcal{D} = \begin{cases} \text{concat}(\mathcal{D}, \rho) & \text{if off-policy} \\ \rho & \text{if on-policy} \end{cases} \quad (32)$$

This method works both for rollouts that contain complete episodes ($d_{n-1} = 1$), and those that contain incomplete episodes ($d_{n-1} \neq 1$, where a rollout might stop before finishing an episode). When combining incomplete episodes with multiple rollout workers, we can experience race conditions. In this specific case, it is easiest to keep one \mathcal{D}, \mathcal{I} per worker.

Upon reaching the maximum capacity of \mathcal{D} , we must discard old transitions to make room for new ones. To make room, we pop the episode begin index from the left of \mathcal{I} and discard the resulting episode in \mathcal{D}

$$\mathcal{I} = \mathcal{I}[1:] \quad (33)$$

$$\mathcal{D} = \mathcal{D}[\mathcal{I}[0]:], \quad (34)$$

where $A[a:] = A[a], A[a+1], \dots$ is array slice notation. We repeat this process until \mathcal{D} can fit the new episodes. Popping \mathcal{I} from the left discards the oldest episode.

5.2. Sampling

Once we have constructed \mathcal{D}, \mathcal{I} , we are ready to train a policy. If we are training on-policy, we can simply train on \mathcal{D} . If we are training off-policy, we want to randomly sample a training batch \mathcal{B} from our dataset. We randomly sample pairs of indices $\{(j, j+1) \mid 0 \leq j < \text{card}(\mathcal{I})\}$ without replacement. We slice \mathcal{D} using these indices to retrieve a random full episode. We continue this process, concatenating our slices together until they reach the user-defined batch size B , truncating the final episode if necessary (Figure 2).

$$\mathcal{B} = \begin{cases} \text{concat}(\mathcal{B}, \mathcal{D}[\mathcal{I}[j] : \mathcal{I}[j+1]]) & \text{if } \text{card}(\mathcal{B}) < B \\ \mathcal{B}[\mathcal{B} : B] & \text{otherwise} \end{cases} \quad (35)$$

where $A[:a] = A[0], A[1], \dots, A[a-1]$. This method ensures we truncate at most one episode per \mathcal{B} . One could extend this approach to implement Prioritized Experience Replay (Schaul et al., 2015) by assigning each index in \mathcal{I} a priority.

5.3. Simplifying the Loss Functions

Unlike SBB, TBB only modifies storage and sampling operations. There is no need to mask outputs or handle additional time dimensions like in SBB. **With TBB, we utilize unmodified, non-recurrent loss functions to train recurrent policies**, reducing the implementation complexity of recurrent RL algorithms. With TBB, the only difference between a recurrent and nonrecurrent update is precomputing the Markov states s, s' before calling the loss function. We demonstrate this by rewriting the DQN update in Algorithm 1, highlighting departures from the non-recurrent version in red.

Algorithm 1 TBB deep Q update

Input: params θ , target params ϕ , Q function Q , sequence model M , train batch \mathcal{B} , discount γ , target update rate β
Output: params θ, ϕ
 $(s_1, s_2, \dots, s_B) \leftarrow M_\theta(T_1, \dots, T_B)$ {Estimate Markov state}
 $(s'_1, s'_2, \dots, s'_B) \leftarrow M_\phi(T_1, \dots, T_B)$ {Next Markov state}
 $\hat{y}_j = r_j + \max_{a \in A} \gamma Q_\phi(s'_j, a), \quad \forall \mathcal{B}[j]$ {Compute target}
 $\theta \leftarrow \min_\theta \|Q_\theta(s_j, a_j) - \hat{y}_j\|, \quad \forall \mathcal{B}[j]$ {Compute loss, update}
 $\phi \leftarrow \phi\beta + (1 - \beta)\theta$ {Update target params}

For posterity, we demonstrate the standard SBB DQN update in Algorithm 2. Note that the update equation has an additional time dimension k and requires mask $m_{i,j}$.

Algorithm 2 SBB deep Q update

Input: params θ , target params ϕ , Q function Q , sequence model M , train batch \mathcal{B} , discount γ , target update rate β
Output: params θ, ϕ

$$\begin{bmatrix} s_{1,1}, \dots, s_{1,L} \\ \vdots \\ s_{B,1}, \dots, s_{B,L} \end{bmatrix} \leftarrow \begin{bmatrix} M_\theta((T_{1,1}) \dots (T_{1,L})) \\ \vdots \\ M_\theta((T_{B,1}) \dots (T_{B,L})) \end{bmatrix}$$

$$\begin{bmatrix} s'_{1,1}, \dots, s'_{1,L} \\ \vdots \\ s'_{B,1}, \dots, s'_{B,L} \end{bmatrix} \leftarrow \begin{bmatrix} M_\phi((T_{1,1}) \dots (T_{1,L})) \\ \vdots \\ M_\phi((T_{B,1}) \dots (T_{B,L})) \end{bmatrix}$$
 $\hat{y}_{j,k} = (r_{j,k} + \max_{a \in A} \gamma Q_\phi(s'_{j,k}, a)), \quad \forall \mathcal{B}[j, k]$
 $\theta \leftarrow \min_\theta m_{j,k} \cdot \|Q_\theta(s_{j,k}, a_{j,k}) - \hat{y}_{j,k}\|, \quad \forall \mathcal{B}[j, k]$
 $\phi \leftarrow \phi\beta + (1 - \beta)\theta$

6. Experiments and Discussion

We begin our experiments with investigating the shortcomings of SBB, specifically the theoretical issues stemming from truncated BPTT. We then compare TBB to SBB across a variety of tasks and models. Finally, we examine the wall-clock efficiency of memory monoids.

All of our experiments utilize tasks from the POPGym benchmark (Morad et al., 2023a), and all TBB to SBB comparisons use identical hyperparameters and random seeds. We validate our findings across State Space Models (S5), Linear Recurrent Units (LRU), Fast and Forgetful Memory (FFM), and the Linear Transformer (LinAttn) memory monoids.

What are the Consequences of Truncating BPTT? We aim to answer whether the estimated (truncated) gradient used in SBB is close to the true gradient. Although there is no theoretical justification for why they should be close, one could imagine that observations made outside the segment are from long ago, and would have little impact on the Q value.

We approach this question by measuring the impact each observation has on the terminal Q value of an episode. In Repeat Previous, the agent must output an observation

from ten timesteps ago – any observations older than ten timesteps are not necessary and, given a relative-time policy, should have little to no impact on the Q function. Recall that we can write the memory model as $s_n = M(o_0, \dots, o_n)$. We explicitly compute

$$\left| \frac{\partial Q(s_n, a_n)}{\partial o_i} \right| = \left| \frac{\partial Q(s_n, a_n)}{\partial s_n} \frac{\partial s_n}{\partial o_i} \right|, \quad (36)$$

and plot the results for FFM, S5, and LRU models in Figure 3. We also plot results for other model and environment combinations in Appendix B.

Surprisingly, we see that virtually all previous observations significantly affect the Q value, across models and tasks. In other words, **learned recurrent Q functions do not generalize well over time, although policies trained with TBB generalize better**. In one case, roughly 90% of the Q value is produced outside the segment boundaries, where backpropagation cannot reach. One possible explanation for this long-tail gradient distribution is that the memory model is “counting” each observation to accurately predict when the episode terminates. Our findings suggest that **SBB could be a major contributor to the increased difficulty and reduced sample efficiency of recurrent RL**, as we demonstrate in the next experiment.

Is TBB More Sample Efficient? For our second experiment, we measure the difference in sample efficiency between TBB and SBB. There are two reasons that TBB could improve upon SBB sample efficiency: (1) As previously discovered, the truncated gradient used by SBB is often a poor estimate of the true gradient (2) the zero padding used in SBB decreases the “effective” batch size. We note that the cost of zero padding in SBB is equivalent to the cost of real data – it takes up equivalent space in the replay buffer and takes just as much compute to process as real data. We report a few combinations of model and task in Figure 5 and present the full results in Appendix A.

We find that TBB produces a noticeable improvement in sample efficiency over SBB, across all configurations of memory model and environment. Even for large segments lengths $L = 100$, we find a significant gap between SBB and TBB. SBB must make an inherent tradeoff – it can use long segments to improve gradient estimates at the cost of smaller effective batch sizes, or shorter segments to improve the effective batch size at the expense of a worse gradient estimate. In our experiments, larger L in SBB always outperform shorter L , suggesting that the gradient estimation error is the main contributor to SBB’s lackluster performance.

Are Memory Monoids Fast in Practice? In Figure 4, we test the wall-clock efficiency of our discounted return monoid against the standard approach of iterating over

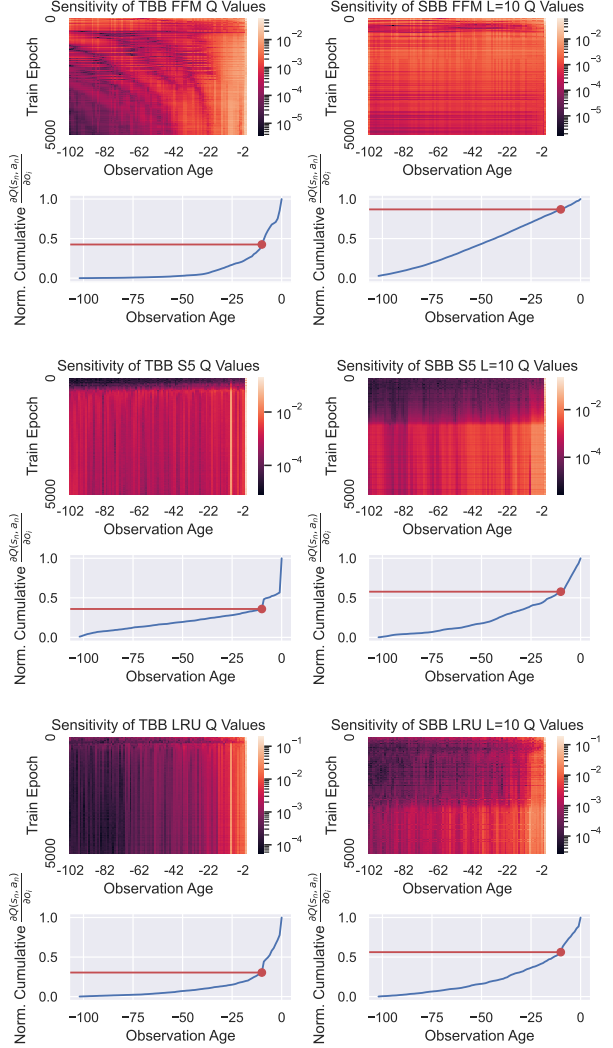


Figure 3. These plots showcase how SBB can hurt Q learning with FFM, S5, and LRU models, even with a segment length L sufficient to capture all necessary information. At the terminal transition of an episode, we compute the partial derivative with respect to the inputs on the Repeat Previous environment, where the agent must output the observation from 10 timesteps ago. **This partial derivative determines how much each prior observation contributes to the Q value.** We also plot the CDF of the partials from the last epoch. The red line and dot correspond to 10 timesteps in the past, the point at which old observations should have no impact on the Q value – but empirically this is not the case. For FFM trained with SBB, **roughly 90% of the Q value is not learnable**, because we cannot backpropagate beyond the segment length of 10. There is no “safe” segment length, in the sense that even the initial observation contributes a nonzero amount to the Q value at the terminal timestep. This emphasizes how important our proposed TBB is, because it enables backpropagation over the entire sequence. We also find that **policies trained with TBB tend to be less sensitive to unnecessary inputs**, suggesting that they generalize better.

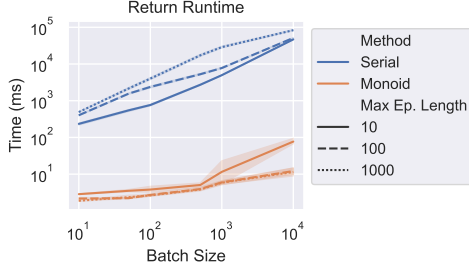


Figure 4. We compare how long it takes to compute the discounted return using our monoid, compared to the standard way of iterating through a batch. Computing the discounted return is orders of magnitude faster when using our monoid implementation. We evaluate ten random seeds on a RTX 2080Ti GPU.

episodes in a batch. Both the monoid and standard approach are just-in-time compiled on a GPU, however the standard approach requires a for loop when the episode lengths are not fixed. We sample a batch of episodes, where each episode length is sampled from a discrete uniform distribution between one and a maximum episode length. We find that our memory monoid computes the discounted return roughly three orders of magnitude faster across the board.

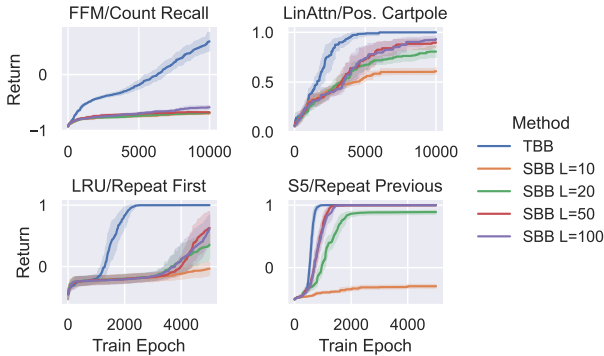


Figure 5. We compare TBB (ours) to SBB across POPGym benchmark tasks and memory models, reporting the mean and 95% bootstrapped confidence interval of the evaluation return over ten seeds. We find that TBB significantly improves sample efficiency.

Next, we compare TBB and SBB scaling. TBB scales worse than SBB ($O(\log B)$ and $O(\log L)$ respectively, where B is the batch size and L is segment length). We question how this overhead translates to wall-clock training time. In Table 1, we examine the total time spent training, finding that the time difference is negligible. The memory model forward pass is only a fraction of the time spent at each epoch, with environment sampling, replay buffer sampling (and in the case of SBB, splitting, truncating, and

padding sequences) all taking a nontrivial amount of time.

Limitations and Future Work According to our sensitivity analysis, old observations unexpectedly impacted the Q value across models and tasks. Beyond the standard sum/product recurrent update rules seen in literature, perhaps there nonlinear update rules that are less sensitive to old information. For example, the max operator could completely overwrite older dimensions of the recurrent state, perhaps focusing more on the present.

In our experiments, we focused on long-term memory tasks from the POPGym benchmark, each of which tests a specific aspect of long-term memory. We did not experiment on environments like Atari, primarily because it is unclear to what extent Atari tasks require long-term memory.

Although memory monoids scale well to long sequences, TBB still pays a $\log B$ time cost. There was no perceptible difference in our experiments, but very long sequences such as those used for in-context RL could incur more noticeable training costs.

7. Related Work

(Lu et al., 2023) provide a resettable scan operator specifically for the S5 model. (Blelloch, 1990) provides a resettable scan for quicksort, but provides no proof nor a general form. (Gu & Dao, 2023) unify a number of linear recurrent models as LTI systems, however, they do not provide a reset mechanism or generalize to non-linear recurrent updates.

There is prior work on special types of experience replay for recurrent models. (Hausknecht & Stone, 2015; Kaputowski et al., 2019) find that warming up segment-based RNNs by replaying older segments can improve the return. However, implementing the warmup is difficult, and it is not clear that warming up the RNN is better than simply increasing the segment size by the warmup length.

8. Conclusion

We introduced memory monoids as a unifying framework for efficient sequence modeling. We found that not only can memory monoids represent a large number of efficient recurrent models, but also the discounted return and the advantage. Given the efficiency of memory monoids over long sequences, we questioned whether the standard truncate-and-pad approach to POMDPs was still necessary. We found that said approach causes both theoretical and practical issues, with shorter segment lengths hampering sample efficiency and ultimately converging to lower returns. We proposed a simple change to batching methodology, that when combined with memory monoids, improves sample efficiency at a negligible cost.

Acknowledgements

We gratefully acknowledge the support of Toshiba Europe Ltd. This work was also supported in part by ARL DCIST CRA W911NF-17-2-0181 and European Research Council (ERC) Project 949940 (gAIa).

References

- Anonymous. Retentive Network: A Successor to Transformer for Large Language Models. In *Submitted to The Twelfth International Conference on Learning Representations*, 2023. URL <https://openreview.net/forum?id=UU9Icwbbhin>.
- Anonymous. TorchRL: A data-driven decision-making library for PyTorch. In *The Twelfth International Conference on Learning Representations*, 2024. URL <https://openreview.net/forum?id=QxItoEAVMb>.
- Bauer, J., Baumli, K., Behbahani, F., Bhoopchand, A., Bradley-Schmieg, N., Chang, M., Clay, N., Collister, A., Dasagi, V., Gonzalez, L., Gregor, K., Hughes, E., Kashem, S., Loks-Thompson, M., Openshaw, H., Parker-Holder, J., Pathak, S., Perez-Nieves, N., Rakicevic, N., Rocktäschel, T., Schroecker, Y., Singh, S., Sygnowski, J., Tuyls, K., York, S., Zacherl, A., and Zhang, L. M. Human-timescale adaptation in an open-ended task space. In Krause, A., Brunskill, E., Cho, K., Engelhardt, B., Sabato, S., and Scarlett, J. (eds.), *Proceedings of the 40th International Conference on Machine Learning*, volume 202 of *Proceedings of Machine Learning Research*, pp. 1887–1935. PMLR, 23–29 Jul 2023. URL <https://proceedings.mlr.press/v202/bauer23a.html>.
- Bellorch, G. E. Prefix Sums and Their Applications. Technical report, School of Computer Science, Carnegie Mellon University, November 1990.
- Bourbaki, N. *Éléments de mathématique. Integration, Livre 1, Livre 5*, 1965. Publisher: Hermann Paris.
- Bradbury, J., Frostig, R., Hawkins, P., Johnson, M. J., Leary, C., Maclaurin, D., Necula, G., Paszke, A., VanderPlas, J., Wanderman-Milne, S., and Zhang, Q. JAX: composable transformations of Python+NumPy programs, 2018. URL <http://github.com/google/jax>.
- Dhulipala, L., Bellorch, G. E., and Shun, J. Theoretically Efficient Parallel Graph Algorithms Can Be Fast and Scalable. *ACM Trans. Parallel Comput.*, 8(1), April 2021. ISSN 2329-4949. doi: 10.1145/3434393. URL <https://doi.org/10.1145/3434393>. Place: New York, NY, USA Publisher: Association for Computing Machinery.
- Gu, A. and Dao, T. Mamba: Linear-time sequence modeling with selective state spaces. *arXiv preprint arXiv:2312.00752*, 2023.
- Gu, A., Johnson, I., Goel, K., Saab, K., Dao, T., Rudra, A., and Ré, C. Combining Recurrent, Convolutional, and Continuous-time Models with Linear State Space Layers. In *Advances in Neural Information Processing Systems*, volume 34, pp. 572–585. Curran Associates, Inc., 2021. URL <https://proceedings.neurips.cc/paper/2021/hash/05546b0e38ab9175cd905eebcc6ebb76-Abstract.html>.
- Gu, A., Goel, K., and Re, C. Efficiently Modeling Long Sequences with Structured State Spaces. March 2022. URL <https://openreview.net/forum?id=uYLFoz1vlAC>.
- Hafner, D., Pasukonis, J., Ba, J., and Lillicrap, T. Mastering Diverse Domains through World Models. *arXiv preprint arXiv:2301.04104*, 2023.
- Hausknecht, M. and Stone, P. Deep Recurrent Q-Learning for Partially Observable MDPs. In *2015 AAAI Fall Symposium Series*, September 2015. URL <https://www.aaai.org/ocs/index.php/FSS/FSS15/paper/view/11673>.
- Huang, S., Dossa, R. F. J., Ye, C., and Braga, J. CleanRL: High-quality Single-file Implementations of Deep Reinforcement Learning Algorithms. 2021. eprint: 2111.08819.
- Kapturowski, S., Ostrovski, G., Quan, J., Munos, R., and Dabney, W. RECURRENT EXPERIENCE REPLAY IN DISTRIBUTED REINFORCEMENT LEARNING. pp. 19, 2019.
- Katharopoulos, A., Vyas, A., Pappas, N., and Fleuret, F. Transformers are RNNs: fast autoregressive transformers with linear attention. In *Proceedings of the 37th International Conference on Machine Learning, ICML’20*, pp. 5156–5165. JMLR.org, July 2020.
- Liang, E., Liaw, R., Nishihara, R., Moritz, P., Fox, R., Goldberg, K., Gonzalez, J., Jordan, M., and Stoica, I. RLlib: Abstractions for distributed reinforcement learning. In *International Conference on Machine Learning*, pp. 3053–3062. PMLR, 2018.
- Lu, C., Schroecker, Y., Gu, A., Parisotto, E., Foerster, J. N., Singh, S., and Behbahani, F. Structured State Space Models for In-Context Reinforcement Learning. In *ICML Workshop on New Frontiers in Learning, Control, and Dynamical Systems*, 2023. URL <https://openreview.net/forum?id=CKPTz21e6k>.
- Morad, S., Kortvelesy, R., Bettini, M., Liwicki, S., and Prorok, A. POPGym: Benchmarking Partially Observable Reinforcement Learning. In *The Eleventh International Conference on Learning Representations*, 2023a. URL <https://openreview.net/forum?id=chDrutUTs0K>.

- Morad, S., Kortvelesy, R., Liwicki, S., and Prorok, A. Reinforcement Learning with Fast and Forgetful Memory. In *Thirty-seventh Conference on Neural Information Processing Systems*, 2023b. URL <https://openreview.net/forum?id=KTfAtro6vP>.
- Orvieto, A., Smith, S. L., Gu, A., Fernando, A., Gulcehre, C., Pascanu, R., and De, S. Resurrecting Recurrent Neural Networks for Long Sequences. In *Proceedings of the 40th International Conference on Machine Learning, ICML'23*. JMLR.org, 2023. Place: Honolulu, Hawaii, USA.
- Peng, B., Alcaide, E., Anthony, Q., Albalak, A., Arcadinho, S., Biderman, S., Cao, H., Cheng, X., Chung, M., Grella, M., GV, K. K., He, X., Hou, H., Lin, J., Kazienko, P., Kocon, J., Kong, J., Koptyra, B., Lau, H., Mantri, K. S. I., Mom, F., Saito, A., Song, G., Tang, X., Wang, B., Wind, J. S., Wozniak, S., Zhang, R., Zhang, Z., Zhao, Q., Zhou, P., Zhou, Q., Zhu, J., and Zhu, R.-J. RWKV: Reinventing RNNs for the Transformer Era, December 2023. URL <http://arxiv.org/abs/2305.13048>. arXiv:2305.13048 [cs].
- Raffin, A., Hill, A., Gleave, A., Kanervisto, A., Ernestus, M., and Dormann, N. Stable-Baselines3: Reliable Reinforcement Learning Implementations. *Journal of Machine Learning Research*, 22(268):1–8, 2021. URL <http://jmlr.org/papers/v22/20-1364.html>.
- Schaul, T., Quan, J., Antonoglou, I., and Silver, D. Prioritized experience replay. *arXiv preprint arXiv:1511.05952*, 2015.
- Schlag, I., Irie, K., and Schmidhuber, J. Linear Transformers Are Secretly Fast Weight Programmers. In *Proceedings of the 38th International Conference on Machine Learning*, pp. 9355–9366. PMLR, July 2021. URL <https://proceedings.mlr.press/v139/schlag21a.html>. ISSN: 2640-3498.
- Schulman, J., Moritz, P., Levine, S., Jordan, M., and Abbeel, P. High-Dimensional Continuous Control Using Generalized Advantage Estimation. In *Proceedings of the International Conference on Learning Representations (ICLR)*, 2016.
- Serrano-Muñoz, A., Chrysostomou, D., Bøgh, S., and Arana-Arexolaleiba, N. skrl: Modular and Flexible Library for Reinforcement Learning. *Journal of Machine Learning Research*, 24(254):1–9, 2023. URL <http://jmlr.org/papers/v24/23-0112.html>.

A. Return Comparison Between TBB and SBB

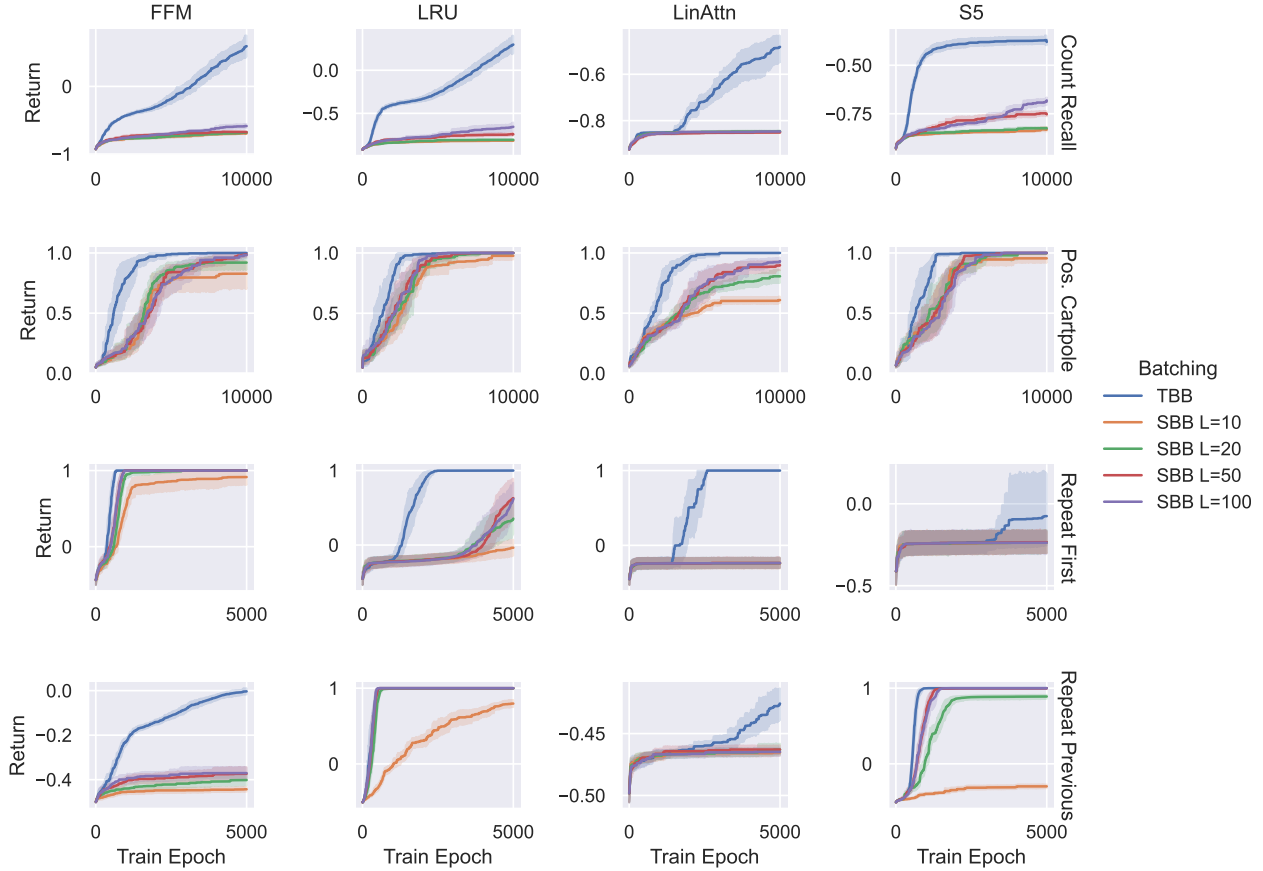


Figure 6. We run four memory monoids on four different POPGym environments over ten seeds and report the mean and 95% bootstrapped confidence interval. The POPGym environments have a minimum episodic return of -1.0 and a maximum of 1.0. In virtually all experiments, Tape-Based Batching provides improved sample efficiency over all tested segments length using Segment-Based Batching. The Count Recall environment has temporal dependencies that span the entire sequence, demonstrating the importance of TBB for long range dependencies. On the other hand, Positional Cartpole has a temporal dependency of two timesteps, and so policies trained via SBB can still do reasonably well. Like Count Recall, Repeat First has long term temporal dependencies, however, SBB-trained methods do better than in Count Recall because Repeat First requires storing and recalling only a single observation.

Method	Total Train Time (s)	Standard Deviation
SBB L=10	886.39	54.47
SBB L=20	886.30	49.71
SBB L=50	887.58	50.29
SBB L=100	886.25	49.87
TBB	886.87	53.21

Table 1. We report the time from start to finish to train a policy, as reported by Wandb. We compare TBB against SBB with various segment lengths, on an RTX 2080Ti. We evaluate FFM, S5, LRU, and Linear Attention over ten seeds on the Repeat First POPGym environment, reporting the mean over all, grouped by batching method. In practice, the performance differences between TBB and SBB seem insignificant.

B. Observation Sensitivity Analysis

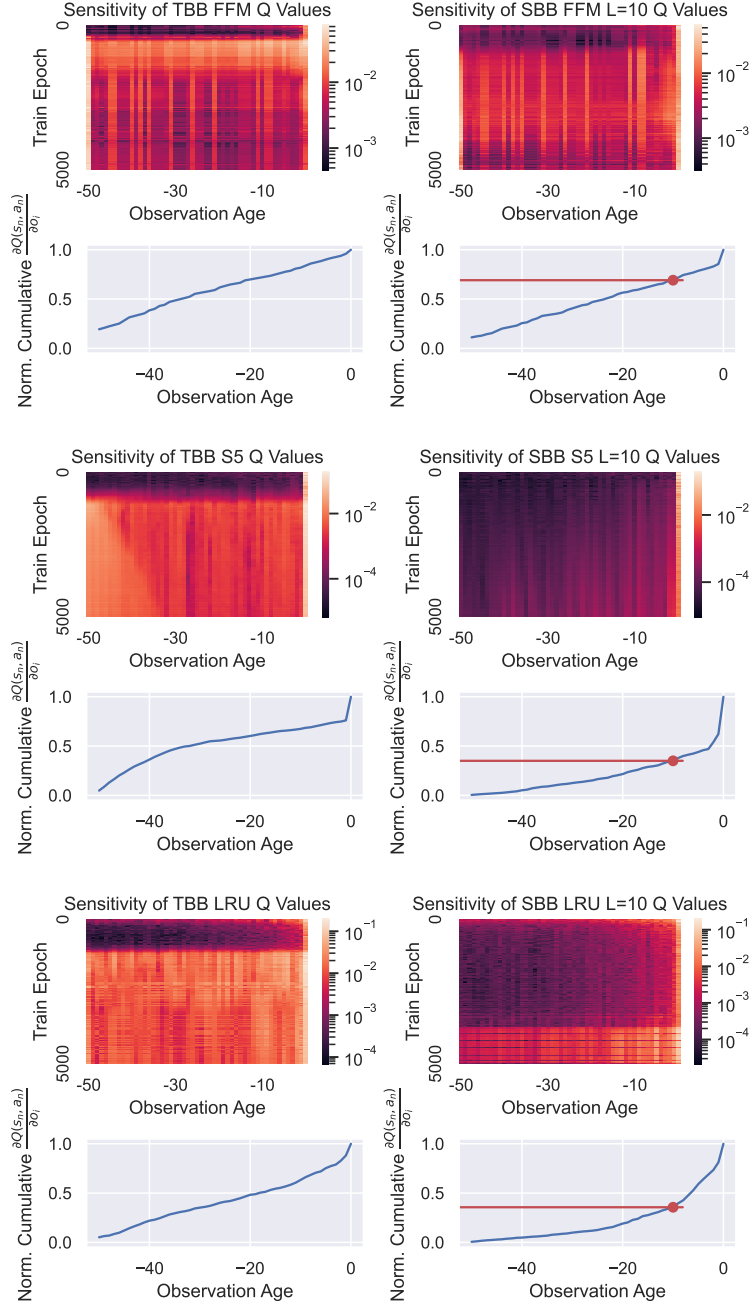


Figure 7. We follow a similar approach to Figure 3 for the Repeat First environment from the POPGym benchmark. At each timestep, the agent receives reward for outputting the initial observation. Unlike Repeat Previous, we expect that the initial observation should have a large contribution to the Q value. We see that for policies trained with TBB, the initial timestep contributes more to Q value than with SBB. In all cases, the Q value is still highly dependent on inputs that are not important.

C. Proofs

Proof of Theorem 3.4. First, let us compute all possible pairs of inputs, as we will use them to simplify the rest of the proof.

$$(A, 0) \circ (A', 0) = (A \cdot (1 - 0) + H_I \cdot 0 \bullet A', 0 \vee 0) = (A \bullet A', 0) \quad (37)$$

$$(A, 1) \circ (A', 0) = (A \cdot (1 - 0) + H_I \cdot 0 \bullet A', 1 \vee 0) = (A \bullet A', 1) \quad (38)$$

$$(A, 0) \circ (A', 1) = (A \cdot (1 - 1) + H_I \cdot 1 \bullet A', 0 \vee 1) = (H_I \bullet A', 1) \quad (39)$$

$$(40)$$

Now, we must demonstrate that associativity holds $((A, b) \bullet (A', b')) \bullet (A'', b'') = (A, b') \bullet ((A', b') \bullet (A'', b''))$ for all possibilities of A, A', A'' and b, b', b'' . That is, we must ensure that the episode boundaries are correctly handled for all possibilities – that information does not leak across episode boundaries and that prior information otherwise propagates forward in time.

$$(A \bullet A', 0) \circ (A'', 0) = ((A \bullet A') \cdot (1 - 0) + H_I \cdot 0 \bullet A'', 0 \vee 0) = (A \bullet A' \bullet A'', 0) \quad (41)$$

$$(A \bullet A', 1) \circ (A'', 0) = ((A \bullet A') \cdot (1 - 0) + H_I \cdot 0 \bullet A'', 1 \vee 0) = (A \bullet A' \bullet A'', 1) \quad (42)$$

$$(H_I \bullet A', 1) \circ (A'', 0) = ((H_I \bullet A') \cdot (1 - 0) + H_I \cdot 0 \bullet A'', 1 \vee 0) = (H_I \bullet A' \bullet A'', 1). \quad (43)$$

And for $b'' = 1$, we have

$$(A \bullet A', 0) \circ (A'', 1) = ((A \bullet A') \cdot (1 - 1) + H_I \cdot 1 \bullet A'', 0 \vee 1) = (A \bullet A' \bullet A'', 1) \quad (44)$$

$$(A \bullet A', 1) \circ (A'', 1) = ((A \bullet A') \cdot (1 - 1) + H_I \cdot 1 \bullet A'', 1 \vee 1) = (H_I \bullet A'', 1) \quad (45)$$

$$(H_I \bullet A', 1) \circ (A'', 1) = ((H_I \bullet A') \cdot (1 - 1) + H_I \cdot 1 \bullet A'', 1 \vee 1) = (H_I \bullet A'', 1). \quad (46)$$

We see that resets correctly remove the impact of any terms that occur before $b' = 1$, while correctly propagating state when $b' = 0$. \square

Proof of Theorem 3.3. We prove the correctness of our discounted return memory monoid by showing the expansion is equivalent to the discounted return.

$$(1, 0) \bullet (\gamma, r_0) = (\gamma, r + 0) = (\gamma, r) \quad (47)$$

$$(1, 0) \bullet (\gamma, r_0) \bullet (\gamma, r_1) = (1 \cdot \gamma \cdot \gamma, 0 + 1 \cdot r_0 + \gamma r_1) = (\gamma^2, r_0 + \gamma r_1) \quad (48)$$

$$(1, 0) \bullet (\gamma, r_0) \bullet \dots \bullet (\gamma, r_n) = (1 \cdot \gamma \cdot \gamma \cdot \dots \cdot \gamma, 1 \cdot r_0 + \gamma r_1 + \dots + \gamma^n r_n) \quad (49)$$

$$= \lim_{n \rightarrow \infty} \left(\gamma^n, \sum_{i=0}^n \gamma^i r_i \right) \quad (50)$$

$$(51)$$

\square

D. Generalized Advantage Estimate as a Memory Monoid

Let us define Generalized Advantage Estimation (GAE) in memory-monoid form:

Theorem D.1. *The GAE target given by*

$$A_t = \sum_{l=0}^{\infty} (\lambda\gamma)^l \delta_{t+l}; \quad \delta_t = r_t + \gamma V(s_{t+1}) - V(s_t) \quad (52)$$

is equivalent to computing M over $\delta_t, \delta_{t+1}, \dots$ for the given memory monoid:

$$H = \{(a, g) \mid a \in [0, 1], g \in \mathbb{R}\} \quad (53)$$

$$H_I = (1, 0) \quad (54)$$

$$(a, g) \bullet (a', g') = (aa', ag' + g) \quad (55)$$

$$f(o, b) = (\gamma\lambda, o) \quad (56)$$

$$g((a, g), (o, b)) = g. \quad (57)$$

Proof. We prove the correctness of our GAE memory monoid by showing the expansion is equivalent to the discounted return. This proof is very similar to the proof of the discounted return.

$$(1, 0) \bullet (\gamma\lambda, \delta_t) = (\gamma\lambda, \delta_t + 0) = (\gamma\lambda, \delta_t) \quad (58)$$

$$(1, 0) \bullet (\gamma\lambda, \delta_t) \bullet (\gamma\lambda, \delta_{t+1}) = (1 \cdot \gamma\lambda \cdot \gamma\lambda, 0 + 1 \cdot \delta + \gamma\lambda\delta_{t+1}) = ((\gamma\lambda)^2, \delta + \gamma\lambda\delta_{t+1}) \quad (59)$$

$$(1, 0) \bullet (\gamma\lambda, \delta_t) \bullet \dots \bullet (\gamma\lambda, \delta_{t+n}) = (1 \cdot \gamma\lambda \cdot \gamma\lambda \cdot \dots \cdot \gamma\lambda, 1 \cdot \delta + \gamma\lambda\delta_{t+1} + \dots + \gamma\lambda^n\delta_{t+n}) \quad (60)$$

$$= \lim_{n \rightarrow \infty} \left((\gamma\lambda)^n, \sum_{l=0}^n (\gamma\lambda)^l \delta_{t+l} \right) \quad (61)$$

□

E. Rewriting Sequence Models as Memory Monoids

In this section, we reformulate existing models used in our experiments as memory monoids. This reformulation is necessary to use inline resets for these models. Prior work (Lu et al., 2023) defines an associate scan operator for the S5 variant of State Space Models. Little work is required to rewrite this in memory monoid form:

$$H = \{(A, a) \mid A \in \mathbb{C}^{m \times m}, a \in \mathbb{R}^{m \times 1}\} \quad (62)$$

$$H_I = (I_m, 0) \quad (63)$$

$$(A, a) \bullet (A', a') = (A'A, A'a + a') \quad (64)$$

$$f(o, b) = (W_A, W_a o) \quad (65)$$

$$g((A, a), (o, b)) = (W_1 \text{GeLU}(W_c a) + b_1) \odot \text{sigmoid}(W_2 \text{GeLU}(W_c a) + b_2) \quad (66)$$

where W_A, W_b, W_c are learnable weights, b_1, b_2 are learnable biases, and I_m is the square identity matrix of size m . The Linear Recurrent Unit (Orvieto et al., 2023) could be roughly described as a theoretical simplification of S5, bringing it closer to classical RNNs. Writing it out as a memory monoid, we see that it is nearly identical to S5, however the weight initialization is different

$$H = \{(A, a) \mid A \in \mathbb{C}^{m \times m}, a \in \mathbb{C}^{m \times 1}\} \quad (67)$$

$$H_I = (I_m, 0) \quad (68)$$

$$(A, a) \bullet (A', a') = (A'A, A'a + a') \quad (69)$$

$$f(o, b) = (W_A, W_a o) \quad (70)$$

$$g((A, a), (o, b)) = \text{MLP}(a) \quad (71)$$

Finally, we can rewrite Fast and Forgetful Memory (FFM) as a memory monoid, with the parallel scans simplifying its implementation and fixing numerical instabilities caused by large positive exponentials over long sequences, as discussed in (Morad et al., 2023b).

$$H = \{(A, t) \mid A \in \mathbb{C}^{m \times c}, t \in \mathbb{Z}\} \quad (72)$$

$$H_I = (0, 0) \quad (73)$$

$$(A, t) \bullet (A', t') = (A \odot \exp(t'(-|\alpha| \oplus i\omega)) + A', t + t') \quad (74)$$

$$f(o, b) = \left(\begin{bmatrix} (W_1 o + b_1) \odot \sigma(W_2 o + b_2) \\ \vdots \\ (W_1 o + b_1) \odot \sigma(W_2 o + b_2) \end{bmatrix}^\top, 1 \right) \quad (75)$$

$$g((A, t), (o, b)) = \text{MLP}(\text{LN}(W_3 [\Re(A) \parallel \Im(A)] + b_3)) \odot \sigma(W_4 o + b_4)(1 - \sigma(W_4 o + b_4)) \odot o \quad (76)$$

where W, b are learnable weights and biases, \Re, \Im extract the real and imaginary part of a complex number, \odot is the elementwise product, \oplus is an outer sum, and $\alpha \in \mathcal{R}^n, \omega \in \mathcal{R}^m$ are learnable parameters. We note that unlike the other examples, FFM is a time-varying recurrence because the recurrent updates depends on t .

F. Non-Recurrent Q Learning

Algorithm 3 Non-recurrent Q learning update

Input: params θ , target params ϕ , Q function Q , train batch \mathcal{B} , discount γ
 $\hat{y}_j = r_j + \max_{a \in A} \gamma Q_\phi(s'_j, a), \quad \forall \mathcal{B}[j]$ {Q Target}
 $\theta \leftarrow \min_\theta \|Q_\phi(s_j, a_j) - \hat{y}_j\|, \quad \forall \mathcal{B}[j]$ {Q update}
 $\phi \leftarrow \phi\beta + (1 - \beta)\theta$ {Target update}

G. TBB Pseudocode

Algorithm 4 Pseudocode for inserting transitions using TBB

Input: List of transitions \mathcal{D} , list of indices \mathcal{I} , buffer size D
Output: List of transitions \mathcal{D} , list of indices \mathcal{I}
 $\rho \leftarrow (T_0, T_1, \dots, T_{n-1})$ {Collect a rollout from the environment}
if on_policy **then**
 $\mathcal{D} \leftarrow \rho$
 $\mathcal{I} \leftarrow \text{where}(b_0, \dots, b_{n-1})$ {Return the indices where $b_i = 1$ (begin flag)}
else
 while $(\mathcal{D} + \text{card}(\rho)) > D$ **do**
 $\mathcal{I} \leftarrow \mathcal{I}[1 :]$ {Buffer full, pop the start index for the oldest episode}
 $\mathcal{D} \leftarrow \mathcal{D}[\mathcal{I}[0] :]$ {Pop the transitions for the oldest episode}
 end while
 $\mathcal{I} \leftarrow \text{concat}(\mathcal{I}, \text{card}(\mathcal{D}) + \text{where}(b_0, \dots, b_{n-1}))$ {Track the indices of episode boundaries within \mathcal{D} where $b_i = 1$ (begin flag)}
 $\mathcal{D} \leftarrow \text{concat}(\mathcal{D}, \rho)$ {Add transitions to dataset/replay buffer}
end if

Algorithm 5 Pseudocode for sampling transitions using TBB

Input: List of transitions \mathcal{D} , list of indices \mathcal{I} , batch size B
Output: Batch of transitions \mathcal{B}
 $\mathcal{B} \leftarrow ()$ {Empty list}
while $\text{len}(\mathcal{B}) < B$ **do**
 $i \sim \mathcal{U}(0, \text{card}(\mathcal{I}) - 1)$ {Randomly sample an index in \mathcal{I} }
 $\mathcal{B} \leftarrow \text{concat}(\mathcal{B}, \mathcal{D}[\mathcal{I}[i] : \mathcal{I}[i + 1]])$ {Append an episode, between two start indices, from the buffer to our batch}
end while
 $\mathcal{B} = \mathcal{B}[: B]$ {Last episode could make batch too large, truncate final episode if necessary}

H. Glossary of Symbols

Symbol	Meaning
S	State space
A	Action space
R	Reward function
\mathcal{T}	State transition function
γ	Discount factor
s	Markov state
a	action
r	reward
s'	next state
d	Done flag
b	Begin flag
\mathcal{O}	Observation function
O	Observation space
o	Observation
T	Transition (o, a, r, o', d, b)
\bar{T}	Partial transition (o, b)
ρ	Rollout
E	Episode of transitions
L	Segment length
\mathcal{D}	Dataset
\mathcal{B}	Train batch
B	Batch size
σ	Segment
m	Boolean mask for segment
\mathcal{L}	Loss function
θ	Model parameters
H	Set of recurrent states
H_I	An identity element in H
\bullet	A monoid binary operator
f	A mapping from a partial transition to H
g	A mapping from H and O to the Markov state S
M	Memory model that summarizes a sequence of transitions
n	Length of a sequence
G	Both the discounted return and the set of resettable monoid recurrent states
G_I	The identity element in G
\circ	A resettable monoid binary operator
\vee	Logical or
pad	An operation that right zero pads a vector to a specified length
split	Splits a long episode into subsequences of length $\leq L$
concat	A vector/matrix concatenation operator
card	The cardinality of the argument

Table 2. A glossary of symbols